Korean J. Chem. Eng., 35(6), 1348-1353 (2018)
DOI: 10.1007/s11814-018-0034-8

pISSN: 0256-1115
eISSN: 1975-7220

Damage to amorphous indium-gallium-zinc-oxide thin film transistors under Cl_2 and BCl_3 plasma

Jong Hoon Choi*, Sung Jin Kim,***, Hyung Tae Kim*, and Sung Min Cho*,†**

*School of Chemical Engineering, Sungkyunkwan University, Suwon 16419, Korea
**School of Semiconductor & Display Engineering, Sungkyunkwan University, Suwon 16419, Korea
***Display Laboratory, Samsung Institute of Technology, Yongin 17113, Korea
(*Received 28 October 2017 • accepted 12 February 2018*)

Abstract−Plasma damage of indium-gallium-zinc-oxide (IGZO) thin film transistor (TFT) was investigated. The IGZO TFT was fabricated and the performance was measured before and after BCl_3 and/or Cl_2 plasma treatment to evaluate the IGZO damage. The BCl_3 and/or Cl_2 plasma deteriorated the IGZO TFT performance significantly even after a short exposure time in the plasma. We propose a new wet etching process to remove a source/drain metal without damaging the underlying IGZO layer. The wet etching process can be utilized for the fabrication of IGZO TFT array using a roll-to-roll process via a self-aligned imprint lithography technique.

Keywords: Indium-gallium-zinc-oxide (IGZO), Thin Film Transistor (TFT), Plasma Damage, Plasma Etching

INTRODUCTION

For large-area and high resolution organic light-emitting diode (OLED) displays, a thin-film-transistor (TFT) requires a semiconductor material with a high carrier mobility. The TFT with metal oxide semiconductors has attracted much attention due to the high carrier mobility and scalability to a large area for the OLED display [1-3]. Among the metal oxide semiconductors, amorphous indium-gallium-zinc oxide (a-IGZO) has been the most studied material because it provides a better switching characteristics and stability for the TFT [4].

A high resolution active-matrix display requires a TFT backplane with a higher resolution. Since the structure with the smallest dimension in the TFT structure is the semiconductor channel, the toughest task realizing such a high resolution TFT is the pattern alignment of the channel during the backplane fabrication process. This alignment problem is not only important in a conventional sheet-to-sheet backplane fabrication process, but also more critical in a roll-to-roll fabrication process.

A self-aligned imprint lithography (SAIL) method [5-8] has been

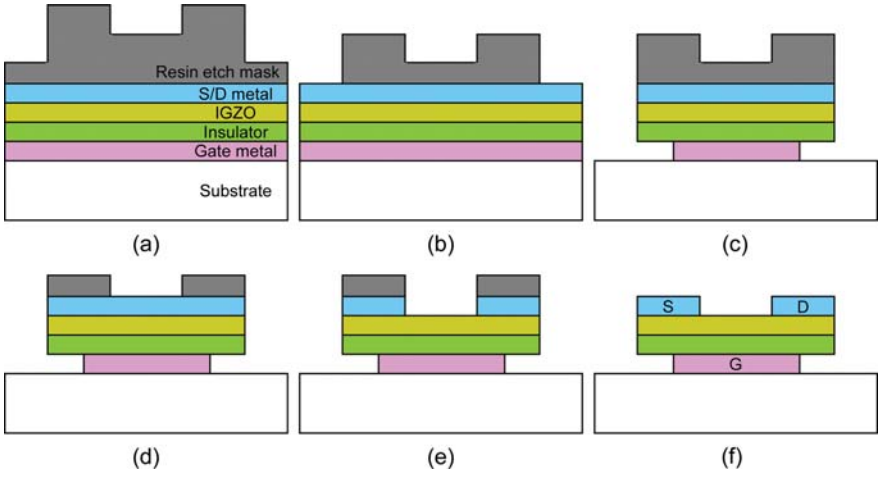

Fig. 1. Schematic diagram of self-aligned imprint lithography (SAIL) process to fabricate a thin film transistor: (a) After the formation of three dimensional etch mask by an imprint lithography; (b) after the first resin mask etching; (c) after the full plasma etching of the transistor layers and under etching of gate metal; (d) after the second resin mask etching; (e) after the S/D metal etching; (f) after the removal of the third resin mask.

†To whom correspondence should be addressed.
E-mail: sungmcho@skku.edu

proposed to implement a high resolution TFT backplane in a roll-to-roll process. Conventional TFTs are fabricated by a series of deposition and pattern-formation processes starting with a substrate (bottom-up method), whereas the SAIL process utilizes a series of etching processes to fabricate the final TFT structure by using pre-aligned multilayer-pattern masks (top-down method). The pre-aligned multilayer pattern mask can be prepared by an imprint lithography using a three-dimensional mold which contains multiple pattern information. Fig. 1 shows a schematic example of the SAIL process for fabricating a simple TFT structure using the IGZO as a semiconductor. As shown in the figure, the multilayer-etch mask that is formed by an imprint lithography method is sequentially etched to reveal different etch-mask patterns for each processing step. For the structure shown in Fig. 1(c), the gate metal should be under-etched by the plasma-etch method with etching gases having a high selectivity for the gate metal. To complete the final IGZO TFT structure, the source/drain (S/D) metal should be etched away to expose the IGZO channel [Fig. 1(e)]. The plasma etching of the S/D metals mainly utilizes gases containing halogen such as chlorine (Cl_2) and/or boron trichloride (BCl_3). However, extreme care should be taken when the S/D metal is etched under a plasma since the IGZO semiconductor layer is easily damaged in a plasma environment.

In this study, we fabricated etch-back-type bottom-gate TFTs to investigate the damage of IGZO TFT under Cl_2 and/or BCl_3 plasma. While the damaging effect of IGZO under nitrogen (N_2), oxygen, and argon (Ar) plasma has been reported in the literature [9-11], Cl_2 and BCl_3 gases have not yet been studied for the IGZO damage under the plasma. This work helps to elucidate the cause of damage on the IGZO TFT during Cl_2 and/or BCl_3 plasma-etch process. We also propose a new wet etching process for an S/D metal of chrome (Cr) as a method to etch the S/D metal with no damage to the IGZO semiconductor. The proposed wet etching process can make the roll-to-roll SAIL process possible for the realization of the high resolution IGZO TFT array.

EXPERIMENTAL

N-type silicon wafers were thermally oxidized to form 150 nm-thick silicon dioxide, which worked as an insulating layer for the IGZO TFT. The n-type silicon works as the gate electrode for the TFT. The IGZO layer (50 nm) was deposited in a radio-frequency (RF) sputtering equipment. The RF power, Ar flow rate, and pressure for the deposition were 50 W, 20 sccm, and 2.6×10^{-3} torr, respectively. The composition of an amorphous IGZO target was 1 : 1 : 1 (mole percent) for In_2O_3 : Ga_2O_3 : ZnO. The IGZO layer was annealed in rapid thermal annealing (RTA) equipment for 1 hour. The RTA was carried out with N_2 flow rate of 100 sccm at the temperature of 300 °C. Standard photolithography and wet etching processes were used to pattern the TFT using a positive photoresist and diluted hydrochloric acid etchant. The width/length (W/L) channel dimension for the TFT was 1,000/100 μm. For the S/D metal, chrome (Cr, 100 nm) was deposited using thermal evaporation.

The fabricated IGZO TFT was treated for 30 and 60 s under BCl_3/Cl_2, Cl_2, and BCl_3 plasma at 10 and 30 W power. The TFT performance was measured before and after the plasma treatment to confirm the IGZO damage. To investigate the IGZO damage during a wet etching of the Cr S/D metal, we treated the TFT in a commercial Cr wet etchant (CR-7, diluted to 5 vol% with water) for 30 and 60 s and compared the TFT performance before and after the treatment. The performance was measured using a probe station (Agilent 4156C). Scanning electron microscopy (SEM) and X-ray photoelectron spectroscopy (XPS) measurements were carried out to understand the chemical and physical damages caused by the Cl_2 and/or BCl_3 plasma.

RESULTS AND DISCUSSION

Plasma etching of the S/D metal such as Cr or aluminum is mainly carried out with Cl_2 and/or BCl_3. It has been known that

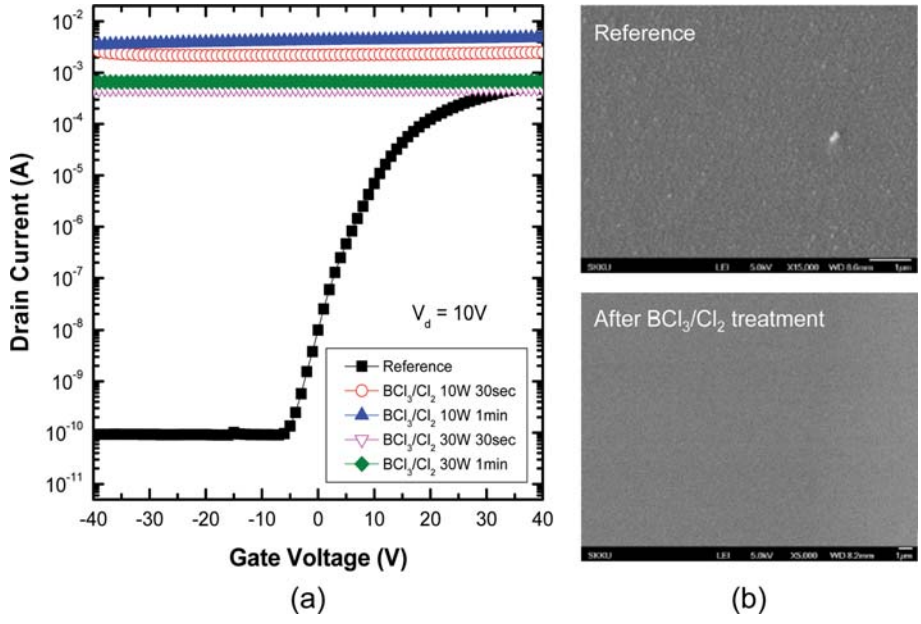

Fig. 2. (a) The changes of the IGZO TFT characteristics and (b) the SEM surface images before and after the BCl_3/Cl_2 plasma treatment.

the Cl_2 gas affects the etch rate of the metal, while the BCl_3 affects the etch selectivity. In this regard, these two gases are utilized separately or simultaneously for the plasma etching of the metals. To investigate the IGZO damage under Cl_2 and/or BCl_3 plasma, we fabricated simple IGZO TFTs and measured their performance before and after the surface of the IGZO channel was exposed under the Cl_2 and/or BCl_3 plasma for 30 and 60 s at 10 and 50 W power. For the reference device, the field-effect mobility, on-off ratio, threshold voltage, and subthreshold swing were 6.3 $cm^2/V{\cdot}s$, 6.85×10^6, 0.43 V, and 2.32 V/decade at the drain voltage of 10 V, respectively.

The devices lost their performance completely after BCl_3/Cl_2 plasma treatment as shown in Fig. 2(a). For the plasma treatment, the chamber pressure was 0.18 torr and the flow rate of BCl_3 and Cl_2 was 20 and 5 sccm, respectively. The devices treated under BCl_3/Cl_2 plasma showed the conducting characteristic regardless of the RF power and treatment time. Fig. 2(b) shows SEM images before and after the plasma treatment of the IGZO surface. From the observation that the grains of a-IGZO surface were fully removed after the plasma treatment, we confirmed that the IGZO was physically etched by the plasma and lost the semiconducting characteristic. Fig. 3 shows the optical microscopy images of the IGZO surface before and after the plasma treatment. The clean IGZO surface of the reference device was damaged after the exposure for 30 s under 10 W BCl_3/Cl_2 plasma. The surface damage became severer after 1 min exposure as shown in Fig. 3(c).

To determine the individual effect of Cl_2 and BCl_3 plasma on the IGZO TFT performance, the exposed IGZO surface was treated separately under Cl_2 and BCl_3 plasma for 30 or 60 s at 10 or 50 W power. The flow rate of Cl_2 or BCl_3 was 20 sccm and the process pressure was 0.15 torr. After the treatment under Cl_2 plasma for 30 s at 10 W, the TFT showed a switching characteristic even though the threshold voltage increased significantly from −0.43 V to −30.8 V. The longer plasma treatment at 10 W power resulted in lower mobility and higher off current. The Cl_2 plasma treatment at 50 W power changed the TFT characteristic to fully conducting because

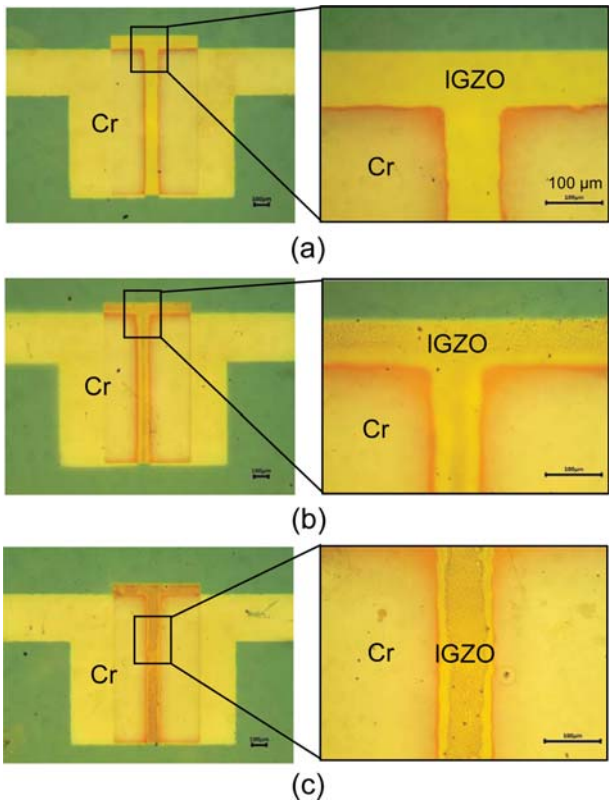

Fig. 3. Optical microscopy images of the IGZO TFT under the BCl_3/Cl_2 plasma at 10 W after (a) 0 s; (b) 30 s; (c) 60 s.

the higher plasma power induced severer physical etching of IGZO due to the stronger ion bombardment. The BCl_3 plasma treatment for 30 s at 10 W power deteriorated the TFT switching characteristic so that the threshold voltage changed from −0.43 V to −21.5 V. However, the TFT switching characteristic disappeared at the longer treatment of 60 s at the same power. It means that the

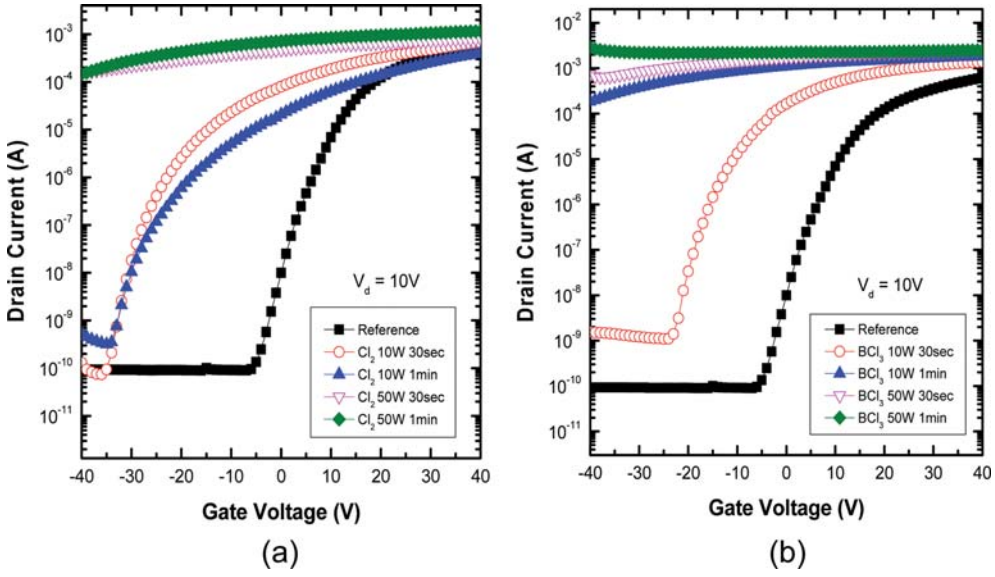

Fig. 4. The changes of the IGZO TFT characteristics before and after (a) Cl_2 and (b) BCl_3 plasma treatment.

BCl_3 plasma treatment not only damages the exposed IGZO surface physically but also chemically. It has been reported [12] that the IGZO can be chemically etched under the BCl_3 plasma. From Figs. 2(a), 4(a), and 4(b), we can conclude that the BCl_3 and Cl_2 plasma can damage the IGZO surface separately, but the plasma damage becomes more severe when the two gases are used together due to their synergetic effect.

Table 1 shows the relative atomic composition of the six elements (In, Ga, Zn, O, B, Cl) in the IGZO surface measured by XPS before and after the BCl_3/Cl_2, Cl_2, and BCl_3 plasma treatments. In all cases, the composition of Cl in the IGZO surface increased significantly due to the Cl radicals in BCl_3 and Cl_2 plasma. Except the Cl_2 plasma treatment, the B atomic composition significantly increased in the IGZO surface due to the BCl_3 plasma. It has been known that $InCl_x$, $ZnCl_x$, Ga_xCl_y, BClO, or B_xO_y could be formed as the result of chemical reactions between the radicals of the etching gas and a-IGZO surface [13]. After the plasma treatment, the atomic percentages of Zn, Ga, and In metals were reduced, as shown in the table. In that the O atomic composition in the surface remains similar for all cases, the relative ratios of the O atom to the each

Table 1. Atomic composition of each element in the IGZO layer measured by XPS before and after the plasma treatment

Treatment	O (%)	B (%)	Cl (%)	Zn (%)	Ga (%)	In (%)
IGZO before treatment	46.77	-	2.11	7.92	34.29	8.92
After BCl_3 10 W	46.06	9.13	7.68	6.09	24.93	6.11
After BCl_3 50 W	45.36	11.56	9.66	5.87	22.04	5.51
After Cl_2 10 W	40.39	-	27.18	6.72	21.09	4.61
After Cl_2 50 W	47.84	-	8.05	9.93	27.16	7.01
After BCl_3/Cl_2 10 W	43.33	11.48	11.95	6.23	21.54	5.48
After BCl_3/Cl_2 50 W	42.52	11.55	13.47	6.5	20.73	5.22

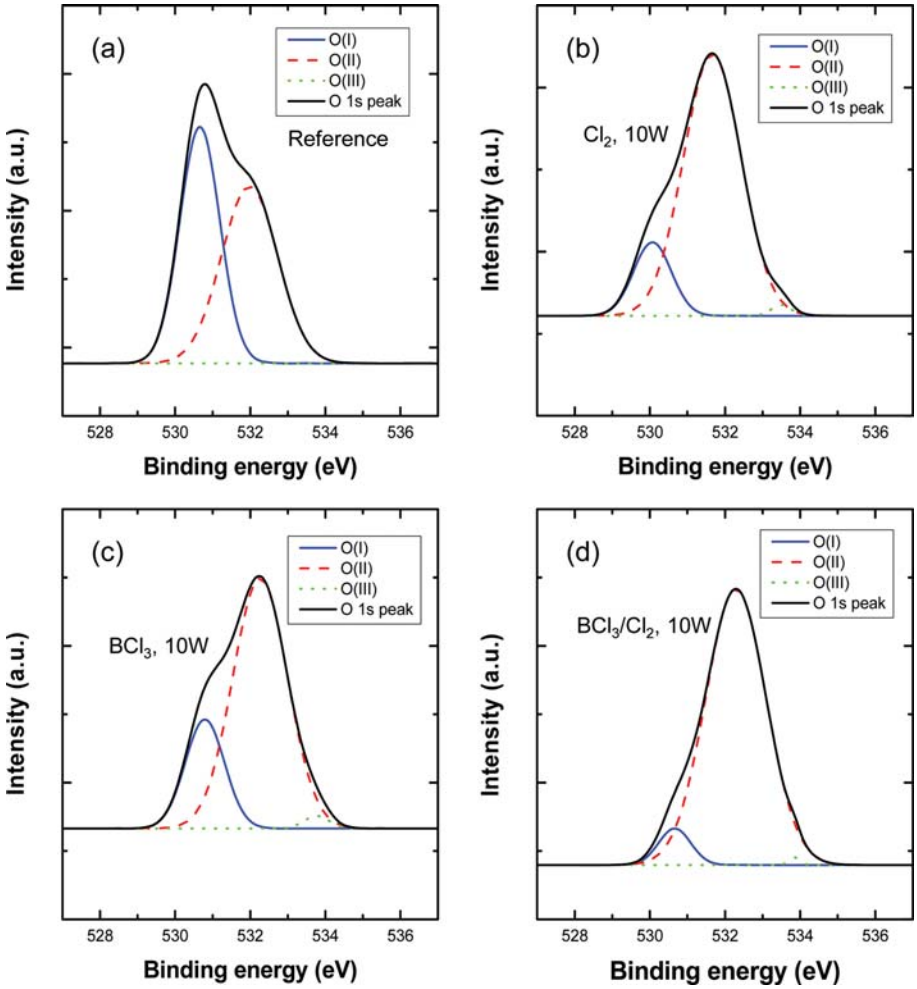

Fig. 5. The O 1s peaks of XPS analysis in a-IGZO channel layer: (a) Before the plasma treatment; (b) after Cl_2 plasma treatment for 30 s; (c) after BCl_3 plasma treatment for 30 s; (d) after BCl_3/Cl_2 plasma treatment for 30 s.

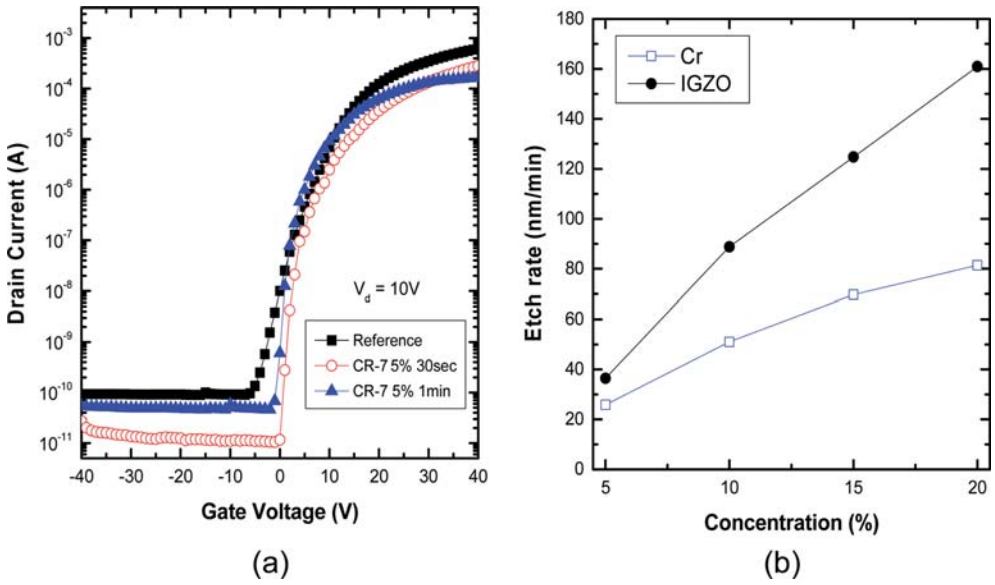

Fig. 6. (a) The changes of the IGZO TFT characteristics before and after the treatment in the diluted CR-7 etching solution; (b) the etching rate of Cr and IGZO layers in the CR-7 etching solution.

metal atom became much higher after the plasma treatments than those before the treatments. Especially, the Ga and In atomic compositions were reduced more significantly than the Zn composition after the plasma treatments. The Ga plays an important role not only to suppress the generation of excessive carriers, but also helps to improve the stability of the IGZO TFT, while the In works for increasing the electron mobility in the IGZO TFT. The decrease in the Ga and In atomic compositions after the plasma treatments should have affected the IGZO TFT characteristics by deteriorating the mobility and stability of the device.

Fig. 5 shows the XPS measurement results of O atom binding energy. It has been known that O 1s spectrum shows three characteristic peaks at 530, 532, and 533 eV. The binding energy peak O(I) at 530 eV represents the O atom bound with metal atoms and the peak O(II) at 532 eV represents the oxygen vacancy of metals to oxygen bonds. A small peak O(III) at 533 eV indicates chemical or physical bonding of IGZO surface with the oxygen-containing molecules such as H_2O, CO_2, or O_2 [13]. As shown in Fig. 5, the relative amount of O atom bound with metals decreased after the plasma treatments, while the relative amount of oxygen vacancy increased on the IGZO surface. Since the oxygen vacancies forms the conducting pathway on IGZO surface, the IGZO TFT showed highly conducting characteristic after the plasma treatments. In case of the BCl_3/Cl_2 plasma treatment, the ratio of the metal-O bond to the metal-O vacancy was the lowest. This result is consistent with the result that the IGZO is damaged the most under the plasma treatment as shown in Figs. 2(a), 4(a) and 4(b).

We showed that the BCl_3 and/or Cl_2 plasma treatments affect the IGZO TFT significantly. Due to the plasma damage of the IGZO surface with BCl_3 and/or Cl_2, it is almost impossible to utilize the plasma etching of the S/D metal layer on the IGZO layer in the SAIL process described in Fig. 1. To remove the S/D metal layer without damaging the IGZO layer, a wet etching process can be implemented instead of the plasma etching. We tested a commercial wet etchant CR-7 for the safe removal of Cr metal for the application. The CR-7 etchant contains perchloric acid ($HClO_4$, 6 wt%), ceric ammonium nitrate [$Ce(NH_4)_2(NO_3)_6$, 9 wt%], and water (85 wt%). Here, the perchloric acid stabilizes chemically ceric ammonium nitrate, which is a strong oxidizing agent. The Cr metal can be etched away by forming chrome nitrate [$Cr(NO_3)_3$] as the result of the chemical reaction between Cr and ceric ammonium nitrate. As shown in Fig. 6, the CR-7 etchant not only etches the Cr metal but also the IGZO. The etch rates depend on the concentration of CR-7 in water. Even though the CR-7 etchant etches the IGZO, the experiment showed that the etchant did not damage the IGZO physically as shown in Fig. 6(a) after treating the exposed IGZO surface in the diluted CR-7 etchant (5 vol% in water).

To realize the SAIL process for the fabrication of the IGZO TFT array using a roll-to-roll process, an S/D metal etching process with no damage to IGZO should be developed. We report that the plasma etching of the S/D metal causes severe damages to the IGZO layer even during a very short process time. Instead of the plasma etching of the S/D metal, we propose the wet etching of the Cr metal on the IGZO layer, which does much less damage to the IGZO layer than plasma etching does. We believe that this new process opens the possibility of the SAIL process for the fabrication of the IGZO TFT array using a roll-to-roll process.

CONCLUSIONS

The IGZO surface was seriously damaged chemically and physically under BCl_3 and/or Cl_2 plasma even after a short exposure time. The plasma damage was confirmed by measuring the degradation of the IGZO TFT performance after the plasma treatments. The chemical and physical changes of the IGZO surface after the plasma treatment were measured by SEM and XPS analyses. After the plasma treatments, the relative amount of oxygen vacancies on the IGZO surface increased and as a result the IGZO TFT lost the

switching characteristics. We proposed a new wet etching process to remove the S/D metal without damaging the underlying IGZO layer.

ACKNOWLEDGEMENTS

This research was supported by the MSIP (Ministry of Science, ICT and Future Planning), Korea, under the ITRC (Information Technology Research Center) support program (IITP-2017-2012-0-00542) supervised by the IITP (Institute for Information & communications Technology Promotion).

REFERENCES

1. E. Fortunato, P. Barquinha and R. Martins, *Adv. Mater.*, **24**, 2945 (2014).
2. T. Kamiya, K. Nomura and H. Hosono, *Sci. Technol. Adv. Mater.*, **11**, 044305 (2010).
3. J. S. Park, W.-J. Maeng, H.-S. Kim and J.-S. Park, *Thin Solid Films*, **520**, 1679 (2012).
4. J. Y. Bak, S. Yang, M. K. Ryu, S. H. Ko Park, C. S. Hwang and S. M. Yoon, *ACS Appl. Mater. Interfaces*, **4**, 5369 (2012).
5. H.-J. Kim, M. Almanza-Workman, B. Garcia, O. Kwon, F. Jeffrey, S. Braymen, J. Hauschildt, K. Junge, D. Larson, D. Stieler, A. Chaiken, B. Cobene, R. Elder, W. Jackson, M. Jam, A. Jeans, H. Luo, P. Mei, C. Perlov and C. Taussig, *J. SID*, **17**, 963 (2009).
6. S. Li and D. Chu, *Flex. Print. Electron.*, **2**, 013002 (2017).
7. E. Lausecker, Y. Huang, T. Fromherz, J. C. Sturm and S. Wagner, *Appl. Phys. Lett.*, **96**, 263501 (2010).
8. P. Mei, M. Almanza-Workman, A. Chaiken, R. L. Cobene, R. Elder, B. Garcia, W. Jackson, M. Jam, A. Jeans, H. J. Kim, O. Kwon, H. Luo, C. Perlov and C. Taussig, *J. Nanosci. Nanotechnol.*, **10**, 7419 (2010).
9. J.-S. Park, J. K. Jeong, Y.-G. Mo, H. D. Kim and S.-I. Kim, *Appl. Phys. Lett.*, **90**, 262106 (2007).
10. J.-S. Kim, M.-K. Joo, M. X. Piao, S.-E. Ahn, Y.-H. Choi, H.-K. Jang and G.-T. Kim, *J. Appl. Phys.*, **115**, 114503 (2014).
11. P. K. Nayak, M. N. Hedhili, D. Cha and H. N. Alshareef, *Appl. Phys. Lett.*, **100**, 202106 (2012).
12. W. Park, K.-W. Whang, Y. G. Yoon, J. H. Kim, S.-H. Rha and C. S. Hwang, *Appl. Phys. Lett.*, **99**, 062110 (2011).
13. Y.-H. Joo, J.-C. Woo and C.-I. Kim, *J. Electrochem. Soc.*, **159**, D190 (2012).